Chapter 8 Flow in Conduits

Entrance and developed flows

Fig. 6.6 Developing velocity profiles and pressure changes in the entrance of a duct flow.

$$Le = f(D, V, \rho, \mu)$$

Π_i theorem $\Rightarrow$ Le/D = f(Re)

Laminar flow: $Re_{crit} \sim 2000$, i.e., for $Re < Re_{crit}$ laminar

$Re > Re_{crit}$ turbulent

Le/D = .06Re   from experiments
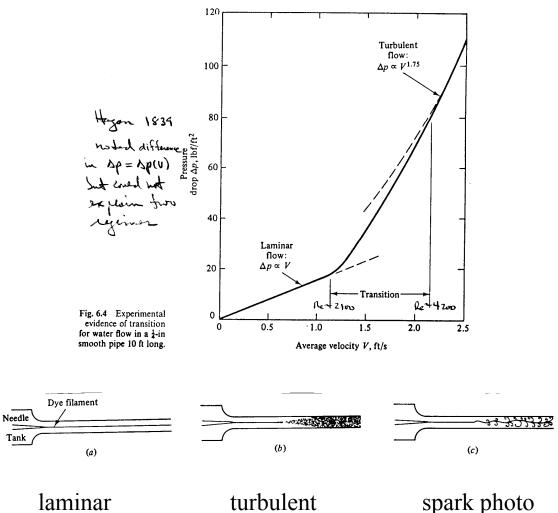
$Le_{max} = .06 Re_{crit} D \sim 138D$

maximum Le for laminar flow

Turbulent flow:

$$\frac{Le}{D} \sim 4.4 \, Re^{1/6}$$

from experiment

Re	Le/D	
4000	18	i.e.,
10^4	20	relatively
10^5	30	shorter
10^6	44	than for
10^7	65	laminar
10^8	95	flow

Laminar vs. Turbulent Flow

Heyen 1839

noted difference
in $\Delta p = \Delta p(v)$
but could not
explain two
regimes

Fig. 6.4 Experimental evidence of transition for water flow in a ½-in smooth pipe 10 ft long.

laminar   turbulent   spark photo

Reynolds 1883 showed difference depends on $Re = \dfrac{VD}{\nu}$

Shear-Stress Distribution Across a Pipe Section
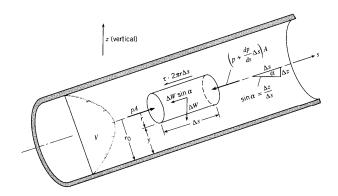

FIGURE 10.1
*Variation of shear stress
in a pipe.*

Continuity: $Q_1 = Q_2 = $ constant, i.e., $V_1 = V_2$ since $A_1 = A_2$

Momentum:
$$\sum F_s = \sum \rho u (\underline{V} \cdot \underline{A})$$
$$= \rho V_1 (-V_1 A_1) - \rho V_2 (V_2 A_2)$$
$$= \rho Q (V_2 - V_1) = 0$$

$$pA - \left(p + \frac{dp}{ds} ds \right) A - \Delta W \sin\alpha - \tau (2\pi r) ds = 0$$

$$\Delta W = \gamma A ds \qquad \sin\alpha = \frac{dz}{ds}$$

$$-\frac{dp}{ds} ds A - \gamma A ds \frac{dz}{ds} - \tau (2\pi r) ds = 0$$

$\div$ Ads

$$\tau = \frac{r}{2} \left[-\frac{d}{ds} (p + \gamma z) \right] \qquad \tau_W = \frac{r_0}{2} \left[-\frac{d}{ds} (p + \gamma z) \right]$$

τ varies linearly from 0.0 at $r = 0$ (centerline) to τ_{max} $(= \tau_w)$ at $r = r_0$ (wall), which is valid for laminar and turbulent flow.

Laminar Flow in Pipes

$$\tau = \mu \frac{dV}{dy} = -\mu \frac{dV}{dr} = \frac{r}{2}\left[-\frac{d}{ds}(p + \gamma z) \right]$$

$$y = \text{wall coordinate} = r_o - r \Rightarrow \frac{dV}{dr} = \frac{dV}{dy}\frac{dy}{dr} = -\frac{dV}{dy}$$

$$\frac{dV}{dr} = -\frac{r}{2\mu}\left[-\frac{d}{ds}(p + \gamma z) \right]$$

$$V = -\frac{r^2}{4\mu}\left[-\frac{d}{ds}(p + \gamma z) \right] + C$$

$$\underbrace{V(r_o) = 0}_{\text{no slip condition}} \Rightarrow C = \frac{r_o^2}{4\mu}\left[-\frac{d}{ds}(p + \gamma z) \right]$$

$$V(r) = \frac{r_o^2 - r^2}{4\mu}\left[-\frac{d}{ds}(p + \gamma z) \right] = V_C\left[1 - \left(\frac{r}{r_0}\right)^2 \right]$$

Exact solution to Navier-Stokes equations for laminar flow in circular pipe

$$\text{where} \quad V_C = \frac{r_o^2}{4\mu}\left[-\frac{d}{ds}(p + \gamma z) \right]$$

$$Q = \int \underline{V} \cdot d\underline{A}$$

$$= \int_0^{r_o} V(r)\underbrace{2\pi r dr}$$

$$dA = r dr d\theta = r dr (2\pi)$$

$$Q = \frac{\pi r_o^4}{8\mu}\left[-\frac{d}{ds}(p+\gamma z)\right] \qquad \overline{V} = \frac{Q}{A} = \frac{r_o^2}{8\mu}\left[-\frac{d}{ds}(p+\gamma z)\right] = \frac{V_C}{2}$$

For a horizontal pipe,

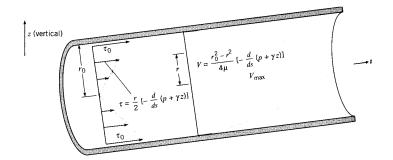$$V_C = \frac{r_o^2}{4\mu}\left[-\frac{d}{ds}(p+\gamma z)\right] = \frac{r_o^2}{4\mu}\frac{\Delta p}{L}$$

where L = length of pipe = ds

$$V(r) = \frac{r_o^2}{4\mu}\frac{\Delta p}{L}\left[1-\left(\frac{r}{r_0}\right)^2\right] = \frac{\Delta p}{4\mu L}\left(r_0^2 - r^2\right)$$

$$Q = \int_0^{r_0} \frac{\Delta p}{2\mu L}\left(r_0^2 - r^2\right)r\,dr = \frac{\pi D^4 \Delta p}{128\mu L}$$

FIGURE 10.2

Distribution of shear stress and velocity for laminar flow in a pipe.

Energy equation:

$$\frac{p_1}{\gamma} + \frac{V_1^2}{2g} + z_1 = \frac{p_2}{\gamma} + \frac{V_2^2}{2g} + z_2 + h_L$$

$$\Delta h = \left(\frac{p_1}{\gamma} + z_1\right) - \left(\frac{p_2}{\gamma} + z_2\right)$$

$$h_L = \frac{p_1 - p_2}{\gamma} + (z_1 - z_2) = \Delta h = L(-\frac{dh}{ds}) = \frac{L}{\gamma}[-\frac{d}{ds}(p + \gamma z)] = \frac{L}{\gamma}[\frac{2\tau_W}{r_0}]$$

Define friction factor $f = \dfrac{8\tau_w}{\rho \overline{V}^2}$ $C_f = \dfrac{\tau_w}{\frac{1}{2}\rho V^2}$

friction coefficient for pipe flow   boundary layer flow

$$h_L = h_f = \frac{L}{\gamma}[\frac{2\tau_W}{r_0}] = \frac{L}{\gamma}[\frac{2(f\rho\overline{V}^2/8)}{r_0}] = f\frac{L}{D}\frac{\overline{V}^2}{2g}$$

Darcy – Weisbach Equation, which is valid for both laminar and turbulent flow.

Friction factor definition based on turbulent flow analysis

where $\tau_w = \tau_w(r_o, \overline{V}, \mu, \rho, k)$ thus n=6, m=3 and r=3 such that $\Pi_{i=1,2,3} = f = \dfrac{8\tau_w}{\rho\overline{V}^2}$,

$Re = \dfrac{\overline{V}D\rho}{\mu} = \dfrac{\overline{V}D}{\nu}$, k/D; or f=f(Re, k/D) where k=roughness height.   For turbulent flow f determined from turbulence modeling since exact solutions not known, as will be discussed next.

For laminar flow f not affected k and f(Re) determined from exact analytic solution to Navier-Stokes equations.

Exact solution:

$$\tau_w = \frac{r_o}{2}\left[-\frac{d}{ds}(p + \gamma z)\right] = \frac{r_o}{2}\left[\frac{8\mu\overline{V}}{r_o^2}\right] = \frac{4\mu\overline{V}}{r_o}$$

For laminar flow $\tau_w = \tau_w(r_o, \overline{V}, \mu)$ thus n=4, m=3 and r=1 such that

$\pi_1 = \dfrac{\tau_W r_o}{\mu \overline{V}}$ =constant. The constant depends on duct shape (circular, rectangular, etc.) and is referred to as Poiseuille number=P_o. P_o=4 for circular duct.

$$f = \frac{32\mu}{\rho r_o \overline{V}} = \frac{64\mu}{\rho \overline{V}D} = \frac{64}{Re}$$

or $\quad h_f = h_L = \dfrac{32\mu L \overline{V}}{\gamma D^2}$ $\qquad$ h_f = head loss due to friction

for $\Delta z = 0$: $\Delta p \propto \overline{V}$ as per Hagen!

Stability and Transition

Stability: can a physical state withstand a disturbance and still return to its original state.

In fluid mechanics, there are two problems of particular interest: change in flow conditions resulting in (1) transition from one to another laminar flow; and (2) transition from laminar to turbulent flow.

(1) Example of transition from one to another laminar flow: Centrifugal instability for Couette flow between two rotating cylinders when centrifugal force > viscous force $Ta = \dfrac{r_i c^3 \left(\Omega_i^2 - \Omega_o^2 \right)}{v^2} > \text{Ta}_{cr} = 1708$ $(c = r_0 - r_i \ll r_i)$, which is predicted by small-disturbance/linear stability theory.
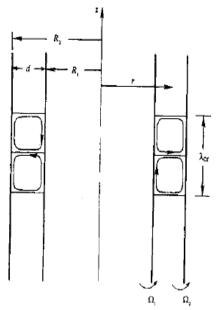

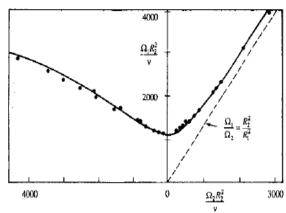Fig. 11.10 Definition sketch of instability in rotating Couette flow.

Fig. 11.11 G. I. Taylor's observation and narrow-gap calculation of marginal stability in rotating Couette flow of water. The ratio of radii is $R_2/R_1 \approx 1.14$. The region above the curve is unstable. The dashed line represents Rayleigh's inviscid criterion, with the region to the left of the line representing instability.

(2)   Transition from laminar to turbulent flow

Not all laminar flows have different equilibrium states, but all laminar flows for sufficiently large Re become unstable and undergo transition to turbulence.

Transition: change over space and time and Re range of laminar flow into a turbulent flow.

$$\mathrm{Re}_{cr} = \frac{U\delta}{\upsilon} \sim 1000,\ \delta = \textit{transverse viscous thickness}$$

$\mathrm{Re}_{trans} > \mathrm{Re}_{cr}$ with $x_{trans} \sim$ 10-20 x_{cr}

Small-disturbance/linear stability theory also predicts Re_{cr} with some success for parallel viscous flow such as plane Couette flow, plane or pipe Poiseuille flow, boundary layers without or with pressure gradient, and free shear flows (jets, wakes, and mixing layers).

No theory for transition, but recent Direct Numerical Simualtions is helpful.

In general: $\mathrm{Re}_{trans} = \mathrm{Re}_{trans}$(geometry, Re, pressure gradient/velocity profile shape, free stream turbulence, roughness, etc.)

Criterion for Laminar or Turbulent Flow in a Pipe

Re_{crit} ~ 2000   flow becomes unstable
Re_{trans} ~ 3000   flow becomes turbulent
$Re = \overline{V}D/\nu$

Turbulent Flow in Pipes

Continuity and momentum:

$$\tau(r = r_o) = \tau_W = \frac{r_o}{2}\left[-\frac{d}{ds}(p + \gamma z)\right]$$

Energy: $h_f = \frac{L}{\gamma}\left[-\frac{d}{ds}(p + \gamma z)\right]$

Combining: $h_f = \frac{L}{\gamma} \cdot \frac{2\tau_W}{r_o}$ define $f = \frac{\tau_W}{\frac{1}{8}\rho \overline{V}^2}$ = friction factor

$$h_f = \frac{L}{\rho g} \cdot \frac{2}{r_o} \cdot \frac{1}{8}\rho \overline{V}^2 f$$

$$h_f = f \cdot \frac{L}{D} \cdot \frac{\overline{V}^2}{2g}   \quad Darcy - Weisbach \ Equation$$

f = f(Re, k/D) = still must be determined!

$$Re = \frac{\overline{V}D}{\nu} \qquad k = roughness$$

Description of Turbulent Flow

Most flows in engineering are turbulent: flows over vehicles (airplane, ship, train, car), internal flows (heating and ventilation, turbo-machinery), and geophysical flows (atmosphere, ocean).

$\underline{V}$ ($\underline{x}$, t) and p($\underline{x}$, t) are random functions of space and time, but statistically stationary flaws such as steady and forced or dominant frequency unsteady flows display coherent features and are amendable to statistical analysis, i.e. time and space (conditional) averaging. RMS and other low-order statistical quantities can be modeled and used in conjunction with averaged equations for solving practical engineering problems.

Turbulent motions range in size from the width in the flow δ to much smaller scales, which come progressively smaller as the Re = Uδ/υ increases.
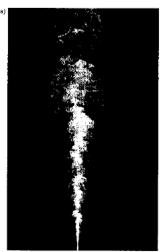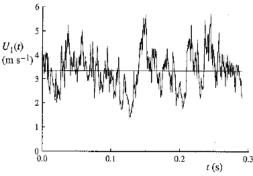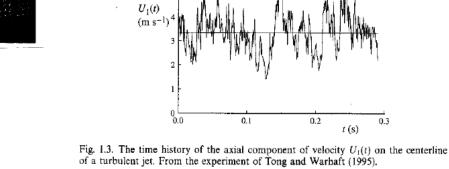
Fig. 1.2. Planar images of concentration in a turbulent jet: (a) Re = 5,000 and (b) Re = 20,000. From Dahm and Dimotakis (1990).

Fig. 1.3. The time history of the axial component of velocity $U_1(t)$ on the centerline of a turbulent jet. From the experiment of Tong and Warhaft (1995).

Fig. 1.1. A photograph of the turbulent plume from the ground test of a Titan IV rocket motor. The nozzle's exit diameter is 3 m, the estimated plume height is 1,500 m, and the estimated Reynolds number is 200×10^6. For more details see Mungal and Hollingsworth (1989). With permission of San Jose Mercury & News.

Fig. 1.4. The mean axial velocity profile in a turbulent jet. The mean velocity $\langle U_1 \rangle$ is normalized by its value on the centerline, $\langle U_1 \rangle_0$; and the cross-stream (radial) coordinate x_2 is normalized by the distance from the nozzle x_1. The Reynolds number is 95,500. Adapted from Hussein, Capp, and George (1994).

Physical description:

(1) Randomness and fluctuations:
       Turbulence is irregular, chaotic, and unpredictable. However, for statistically stationary flows, such as steady flows, can be analyzed using Reynolds decomposition.

$$u = \bar{u} + u' \quad \bar{u} = \frac{1}{T} \int_{t_0}^{t_0+T} u \, dT \quad \bar{u}' = 0 \quad \bar{u'^2} = \frac{1}{T} \int_{t_0}^{t_0+T} u'^2 \, dT \quad \text{etc.}$$

$\bar{u}$ = mean motion
u' = superimposed random fluctuation
$\bar{u'^2}$ = Reynolds stresses; RMS = $\sqrt{\bar{u'^2}}$

Triple decomposition is used for forced or dominant frequency flows

$$u = \bar{u} + u'' + u'$$

Where u'' = organized component

(2) Nonlinearity
       Reynolds stresses and 3D vortex stretching are direct result of nonlinear nature of turbulence. In fact, Reynolds stresses arise from nonlinear convection term after substitution of Reynolds decomposition into NS equations and time averaging.

(3) Diffusion

Large scale mixing of fluid particles greatly enhances diffusion of momentum (and heat), i.e.,

Reynolds Stresses: $\qquad -\rho\overline{u'_i u'_j} \gg \overbrace{\tau_{ij} = \mu\varepsilon_{ij}}^{\textit{viscous stress}}$

Isotropic eddy viscosity: $\quad -\overline{u'_i u'_j} = \nu_t \varepsilon_{ij} - \dfrac{2}{3}\delta_{ij}k$

(4) Vorticity/eddies/energy cascade

Turbulence is characterized by flow visualization as eddies, which vary in size from the largest L_δ (width of flow) to the smallest. The largest eddies have velocity scale U and time scale L_δ/U. The orders of magnitude of the smallest eddies (Kolmogorov scale or inner scale) are:

L_K = Kolmogorov micro-scale = $\left[\dfrac{\nu^3 L_\delta}{U^3}\right]^{\frac{1}{4}} = (\nu^3/\varepsilon)^{1/4}$

$L_K = $ O(mm) $\gg L_{\text{mean free path}} = 6 \times 10^{-8}$ m
Velocity scale = $(\nu\varepsilon)^{1/4}$ = O(10^{-2}m/s)
Time scale = $(\nu/\varepsilon)^{1/2}$ = O(10^{-2}s)

Largest eddies contain most of energy, which break up into successively smaller eddies with energy transfer to yet smaller eddies until L_K is reached and energy is dissipated at rate ε by molecular viscosity.

Richardson (1922):

L_δ Big whorls have little whorls
       Which feed on their velocity;
       And little whorls have lesser whorls,
L_K And so on to viscosity (in the molecular sense).

(5) Dissipation

$$\ell_0 = L_\delta$$

$$u_0 = \sqrt{k} \qquad k = \overline{u'^2} + \overline{v'^2} + \overline{w'^2}$$

$$= 0(U)$$

$$\text{Re}_\delta = u_0 \ell_0 / \upsilon = big$$

Energy comes from largest scales and fed by mean motion

ε = rate of dissipation = energy/time

$$= u_0^2 \Big/ \tau_o \qquad \tau_o = \ell_0 \Big/ u_0$$

Dissipation occurs at smallest scales

$$= u_0^3 \Big/ l_0 \quad \text{independent } \upsilon \qquad L_K = \left[\frac{\upsilon^3}{\varepsilon} \right]^{\frac{1}{4}}$$

The mathematical complexity of turbulence entirely precludes any exact analysis. A statistical theory is well developed; however, it is both beyond the scope of this course and not generally useful as a predictive tool. Since the time of Reynolds (1883) turbulent flows have been analyzed by considering the mean (time averaged) motion

and the influence of turbulence on it; that is, we separate the velocity and pressure fields into mean and fluctuating components.

It is generally assumed (following Reynolds) that the motion can be separated into a mean $(\overline{u}, \overline{v}, \overline{w}, \overline{p})$ and superimposed turbulent fluctuating (u', v', w', p') components, where the mean values of the latter are 0.

$$u = \overline{u} + u' \qquad\qquad p = \overline{p} + p'$$
$$v = \overline{v} + v' \qquad\qquad \text{and for compressible flow}$$
$$w = \overline{w} + w' \qquad\qquad \rho = \overline{\rho} + \rho' \text{ and } T = \overline{T} + T'$$

where (for example)

$$\overline{u} = \frac{1}{t_1} \int_{t_0}^{t_0 + t_1} u\, dt$$

and t_1 sufficiently large that the average is independent of time

Thus by definition $\overline{u'} = 0$, etc. Also, note the following rules which apply to two dependent variables f and g

$$\overline{\overline{f}} = \overline{f} \qquad \overline{f + g} = \overline{f} + \overline{g}$$

$$\overline{\overline{f} \cdot g} = \overline{f} \cdot \overline{g}$$

$$\overline{\frac{\partial f}{\partial s}} = \frac{\partial \overline{f}}{\partial s} \qquad \overline{\int f ds} = \int \overline{f} ds \qquad\qquad \begin{array}{l} f = (u, v, w, p) \\ s = (x, y, z, t) \end{array}$$

The most important influence of turbulence on the mean motion is an increase in the fluid stress due to what are

called the apparent stresses. Also known as Reynolds stresses:

$$\tau'_{ij} = -\rho\overline{u'_i u'_j}$$

$$= \begin{bmatrix} -\rho\overline{u'^2} & -\rho\overline{u'v'} & -\rho\overline{u'w'} \\ -\rho\overline{u'v'} & -\rho\overline{v'^2} & -\rho\overline{v'w'} \\ -\rho\overline{u'w'} & -\rho\overline{v'w'} & -\rho\overline{w'^2} \end{bmatrix} \quad \begin{array}{l} \text{Symmetric} \\ 2^{\text{nd}} \text{ order} \\ \text{tensor} \end{array}$$

The mean-flow equations for turbulent flow are derived by substituting $\underline{V} = \overline{\underline{V}} + \underline{V}'$ into the Navier-Stokes equations and averaging. The resulting equations, which are called the Reynolds-averaged Navier-Stokes (RANS) equations are:

Continuity $\nabla \cdot \underline{V} = 0$ i.e. $\nabla \cdot \overline{\underline{V}} = 0$ and $\nabla \cdot \underline{V}' = 0$

Momentum $\rho\dfrac{D\overline{V}}{Dt} + \rho\dfrac{\partial}{\partial x_j}\left(\overline{u'_i u'_j}\right) = -\rho g\hat{k} - \nabla\overline{p} + \mu\nabla^2\underline{\overline{V}}$

or $\rho\dfrac{D\overline{V}}{Dt} = -\rho g\hat{k} - \nabla\overline{p} + \nabla \cdot \tau_{ij}$

$$\tau_{ij} = \mu\left[\dfrac{\partial u_i}{\partial x_j} + \dfrac{\partial u_j}{\partial x_i}\right] - \underbrace{\rho\overline{u'_i u'_j}}_{\tau'_{ij}}$$

$u_1 = u \qquad x_1 = x$
$u_2 = v \qquad x_2 = y$
$u_3 = w \qquad x_3 = z$

Comments:

1) equations are for the mean flow
2) differ from laminar equations by Reynolds stress
   terms $= -\rho\overline{u_i'u_j'}$
3) influence of turbulence is to transport momentum
   from one point to another in a similar manner as
   viscosity
4) since $\overline{u_i'u_j'}$ are unknown, the problem is
   indeterminate: the central problem of turbulent flow
   analysis is closure!
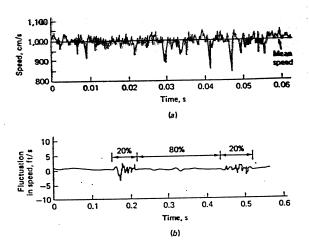
4 equations and $4 + 6 = 10$ unknowns

FIGURE 5-35
Hot-wire measurements showing turbulent velocity fluctuations: (a) typical
trace of a single velocity component in a turbulent flow; (b) trace showing
intermittent turbulence at the edge of a jet.

FIGURE 5-36
Flat-plate measurements of the fluctuating velocities u' (streamwise),
(normal), and w' (lateral) and the turbulent shear $u'v'$. [After Klebanoff (1955).]
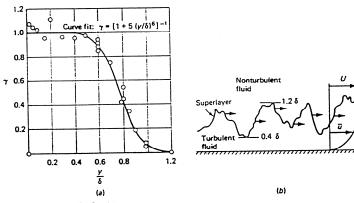
FIGURE 5-37
The phenomenon of intermittency in a turbulent boundary layer: (a) measured intermittency factors [after Klebanoff (1955)]; (b) the superlayer interface between turbulent and nonturbulent fluid.
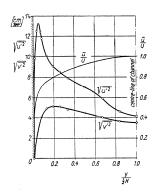
$$\psi = \frac{\overline{u'\,v'}}{\sqrt{\overline{u'^2}} \cdot \sqrt{\overline{v'^2}}}$$

Fig. 18.3. Measurement of fluctuating turbulent components in a wind tunnel, at maximum velocity $U = 100$ cm/sec after Reichardt [41]

Root-mean-square of longitudinal fluctuation $\sqrt{\overline{u'^2}}$, transverse fluctuation $\sqrt{\overline{v'^2}}$, mean velocity $\bar{u}$
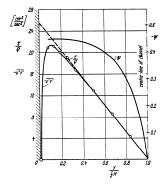
Fig. 18.4. Measurement of fluctuating components in a channel, after Reichardt [41]

The product $\overline{u'\,v'}$, the shearing stress τ/ϱ, and the correlation coefficient ψ

Turbulence Modeling

Closure of the turbulent RANS equations require the determination of $-\rho\overline{u'v'}$, etc. Historically, two approaches were developed: (a) eddy viscosity theories in which the Reynolds stresses are modeled directly as a function of local geometry and flow conditions; and (b) mean-flow velocity profile correlations, which model the mean-flow profile itself. The modern approaches, which are beyond the scope of this class, involve the solution for transport PDE's for the Reynolds stresses, which are solved in conjunction with the momentum equations.
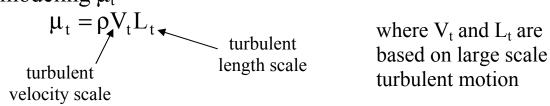
(a) eddy-viscosity: theories

$$-\rho\overline{u'v'} = \mu_t \frac{\partial \overline{u}}{\partial y}$$

In analogy with the laminar viscous stress, i.e., $\tau_t \propto$ mean-flow rate of strain

The problem is reduced to modeling μ_t, i.e.,
$\mu_t = \mu_t(\underline{x}, \text{ flow at hand})$

Various levels of sophistication presently exist in modeling μ_t

$$\mu_t = \rho V_t L_t$$

turbulent velocity scale

turbulent length scale

where V_t and L_t are based on large scale turbulent motion

The total stress is

$$\tau_{total} = (\mu + \mu_t)\frac{\partial \overline{u}}{\partial y}$$

molecular viscosity

eddy viscosity
(for high Re flow $\mu_t \gg \mu$)

Mixing-length theory (Prandtl, 1920)

$$-\rho\overline{u'v'} = c\rho\sqrt{\overline{u'^2}}\sqrt{\overline{v'^2}}$$

based on kinetic theory of gases

$$\sqrt{\overline{u'^2}} = \ell_1\frac{\partial\overline{u}}{\partial y}$$

ℓ_1 and ℓ_2 are mixing lengths which are analogous to molecular mean free path, but much larger

$$\sqrt{\overline{v'^2}} = \ell_2\frac{\partial\overline{u}}{\partial y}$$

$$\Rightarrow\quad -\rho\overline{u'v'} = \rho\,\underbrace{\ell^2\left|\frac{\partial\overline{u}}{\partial y}\right|\frac{\partial\overline{u}}{\partial y}}_{\mu_t}$$

Known as a zero equation model since no additional PDE's are solved, only an algebraic relation

distance across shear layer

$$\ell = \ell(y)$$

= f(boundary layer, jet, wake, etc.)

Although mixing-length theory has provided a very useful tool for engineering analysis, it lacks generality. Therefore, more general methods have been developed.

One and two equation models

$$\mu_t = \frac{C\rho k}{\varepsilon}$$

C = constant

k = turbulent kinetic energy
$$= \overline{u'^2 + v'^2 + w'^2}$$

ε = turbulent dissipation rate

Governing PDE's are derived for k and ε which contain terms that require additional modeling. Although more general than the zero-equation models, the k-ε model also has definite limitation; therefore, relatively recent work involves the solution of PDE's for the Reynolds stresses themselves. Difficulty is that these contain triple correlations that are very difficult to model. Most recent work involves direct and large eddy simulation of turbulence.

 (b)   <u>mean-flow velocity profile correlations</u>

As an alternative to modeling the Reynolds stresses one can model mean flow profile directly for wall bounded flows such as pipes/channels and boundary layers. For simple 2-D flows this approach is quite good and will be used in this course. For complex and 3-D flows generally not successful. Consider the shape of a turbulent velocity profile for wall bounded flow.
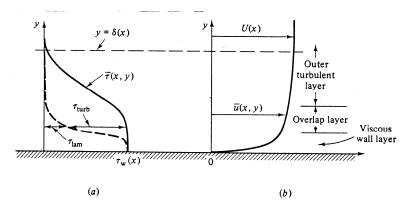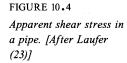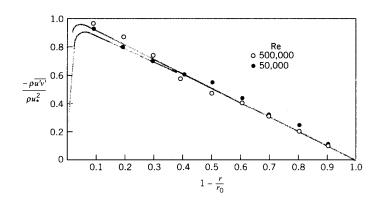
Fig. 6.8 Typical velocity and shear distributions in turbulent flow near a wall: (a) shear; (b) velocity. (measurements)

FIGURE 10.4

Apparent shear stress in a pipe. [After Laufer (23)]

Note that very near the wall τ_{laminar} must dominate since $-\rho\overline{u_i u_j} = 0$ at the wall (y = 0) and in the outer part turbulent stress will dominate. This leads to the three-layer concept:

Inner layer: viscous stress dominates

Outer layer: turbulent stress dominates

Overlap layer: both types of stress important

1. laminar sub-layer (viscous shear dominates)

$$\bar{u} = f(\mu, \tau_w, \rho, y)$$

note: not $f(\delta)$
and $\delta = D$ and
$y = r_o - r$
for pipe flow

From dimensional analysis

$$u^+ = f\left(y^+\right)$$

law-of-the-wall

where:

$$u^+ = \frac{\bar{u}}{u^*}$$

$$u^* = \text{friction velocity} = \sqrt{\tau_w / \rho}$$

$$y^+ = \frac{yu^*}{\nu}$$

very near the wall:

$$\tau \sim \tau_w \sim \text{constant} = \mu \frac{d\bar{u}}{dy} \quad \Rightarrow \quad \bar{u} = cy$$

i.e.,

$$u^+ = y^+ \qquad 0 < y^+ < 5$$

2. outer layer (turbulent shear dominates)

$$\left(\bar{u}_e - \bar{u}\right)_{outer} = g\left(\delta, \tau_w, \rho, y\right)$$

note: independent of μ and actually also depends on $\dfrac{dp}{dx}$

From dimensional analysis

$$\frac{\bar{u}_e - \bar{u}}{u^*} = g\underbrace{\left(\frac{y}{\delta}\right)}_{\eta}$$ velocity defect law

3. <u>overlap layer</u> (viscous and turbulent shear important)

It is not that difficult to show that for both laws to overlap, f and g are logarithmic functions:

Inner region:

$$\frac{d\bar{u}}{dy} = \frac{u^{*2}}{\nu}\frac{df}{dy^+}$$

Outer region:

$$\frac{d\bar{u}}{dy} = \frac{u^*}{\delta}\frac{dg}{d\eta}$$

$$\underbrace{\frac{y}{u^*}\frac{u^{*2}}{\nu}\frac{df}{dy^+}}_{f(y+)} = \underbrace{\frac{y}{u^*}\frac{u^*}{\delta}\frac{dg}{d\eta}}_{g(\eta)}; \text{ valid at large } y^+ \text{ and small } \eta.$$

Therefore, both sides must equal universal constant, κ^{-1}

$$f(y^+) = \frac{1}{\kappa}\ln y^+ + B = \bar{u}/u^* \quad \text{(inner variables)}$$

$$g(\eta) = \frac{1}{\kappa}\ln\eta + A = \frac{\bar{u}_e - \bar{u}}{u^*} \quad \text{(outer variables)}$$

κ, A, and B are pure dimensionless constants

Values vary somewhat depending on different exp. arrangements

κ = 0.41   Von Karman constant

B = 5.5   (or 5.0)

A = 2.35   BL flow   *The difference is due to*
  = 0.65   pipe flow   *loss of intermittency in*
                         duct flow. A = 0 means
                         small outer layer

FIGURE 10.5

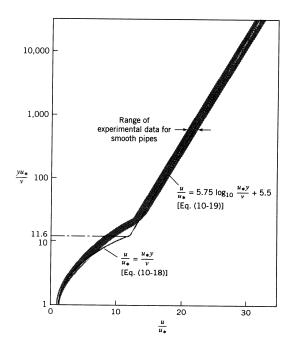*Velocity distribution for smooth pipes. [After Schlichting (36)]*

$$\frac{u}{u_*} = 5.75 \log_{10} \frac{u_* y}{\nu} + 5.5$$
[Eq. (10-19)]

$$\frac{u}{u_*} = \frac{u_* y}{\nu}$$
[Eq. (10-18)]

FIGURE 9.9

Velocity distribution in a turbulent boundary layer.

$$\frac{u}{u_*} = 5.75 \log \frac{y u_*}{\nu} + 5.56$$

$$\frac{y u_*}{\nu} = 11.84$$

$$\frac{u}{u_*} = \frac{u_* y}{\nu}$$

FIGURE 9.11

Velocity distribution in a turbulent boundary layer–linear scales.

FIGURE 9.12

Velocity-defect law for boundary layers. [After Rouse (10)].

Note that the y^+ scale is logarithmic and thus the inner law only extends over a very small portion of δ

Inner law region $< .2\delta$

And the log law encompasses most of the pipe/boundary-layer. Thus as an approximation one can simply assume

$$\frac{\overline{u}}{u^*} = \frac{1}{\kappa}\ln y^+ + B$$

$$u^* = \sqrt{\tau_w / \rho}$$

$$y^+ = \frac{yu^*}{\nu}$$

is valid all across the shear layer. This is the approach used in this course for turbulent flow analysis. The approach is a good approximation for simple and 2-D flows (pipe and flat plate), but does not work for complex and 3-D flows.
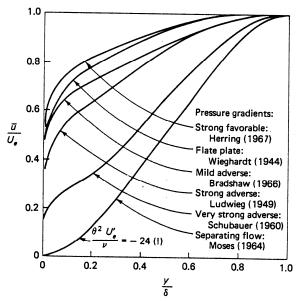

FIGURE 6-4
Experimental turbulent-boundary-layer velocity profiles for various pressure gradients.
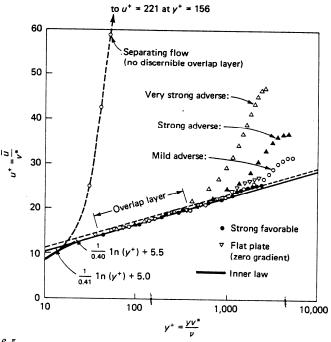
FIGURE 6-5
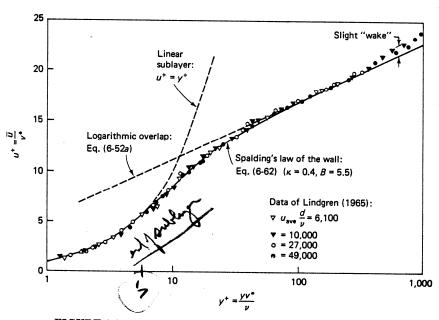Replot of the velocity profiles of Fig. 6-4 using inner-law variables y^+ and u^+.

FIGURE 6-6
Comparison of Spalding's inner-law expression with the pipe-flow data of Lindgren (1965).

Velocity Distribution and Resistance in Smooth Pipes

Assume log-law is valid across entire pipe

$$u^* = \sqrt{\frac{\tau_w}{\rho}} = \text{ friction velocity}$$

$$\frac{\overline{u}(r)}{u^*} = \frac{1}{\kappa} \ln \frac{(r_o - r)u^*}{\nu} + B$$

$$\kappa = .41$$
$$B = 5.0$$

$$\overline{V} = \frac{Q}{A} = \frac{\int_0^{r_o} \overline{u}(r)2\pi r dr}{\pi r_o^2} = \frac{1}{2}u^* \left\{ \frac{2}{\kappa} \ln \frac{r_o u^*}{\nu} + 2B - \frac{3}{\kappa} \right\}$$

drop over bar:
$$\frac{V}{u^*} = 2.44 \ln \underbrace{\frac{r_o u^*}{\nu}}_{\frac{1}{2}Re\left(\frac{f}{8}\right)^{1/2}} + 1.34 = \left(\frac{\rho V^2}{\tau_o}\right)^{1/2} = \left(\frac{8}{f}\right)^{1/2}$$

$$\frac{1}{\sqrt{f}} = 1.99 \log\left(Re\, f^{1/2}\right) - 1.02$$

constants
adjusted $\Rightarrow \dfrac{1}{\sqrt{f}} = 2\log\left(Re\, f^{1/2}\right) - .8$ $Re > 3000$
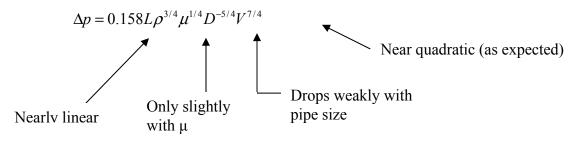using data

Since f equation is implicit, it is not easy to see dependency on ρ, μ, V, and D

$$f(pipe) = 0.316 \, Re_D^{-1/4}$$ $4000 < Re_D < 10^5$
Blasius (1911) power law
curve fit to data

for Δz=0 (horizontal)

$$h_f = \frac{\Delta p}{\gamma} = f \frac{L}{D} \frac{V^2}{2g}$$

$$\Delta p = 0.158 L \rho^{3/4} \mu^{1/4} D^{-5/4} V^{7/4}$$

Near quadratic (as expected)

Nearly linear

Only slightly with μ

Drops weakly with pipe size

$$= 0.241 L \rho^{3/4} \mu^{1/4} D^{-4.75} Q^{1.75}$$

laminar flow: $\Delta p = 8 \mu L Q / \pi R^4$

Δp (turbulent) increases more sharply than Δp (laminar) for same Q; therefore, increase D for smaller Δp. 2D decreases Δp by 27 for same Q.

$$\frac{u_{max}}{u^*} = \frac{u(r=0)}{u^*} = \frac{1}{\kappa} \ln \frac{r_0 u^*}{\upsilon} + B$$

Combine with

$$\frac{V}{u^*} = \kappa^{-1} \ln \frac{r_0 u^*}{\upsilon} + B - \frac{3}{2\kappa}$$

$$\frac{V}{u_{max}} = \left(1 + 1.3\sqrt{f}\right)^{-1}$$

$$1.3 = \frac{3}{2\kappa\sqrt{8}}$$

TABLE 10.1   EXPONENTS FOR POWER-LAW EQUATION AND
RATIO OF MEAN TO MAXIMUM VELOCITY

Re →	4×10^3	2.3×10^4	1.1×10^5	1.1×10^6	3.2×10^6
$m \rightarrow$	$\dfrac{1}{6.0}$	$\dfrac{1}{6.6}$	$\dfrac{1}{7.0}$	$\dfrac{1}{8.8}$	$\dfrac{1}{10.0}$
$\overline{V}/V_{max} \rightarrow$	0.791	0.807	0.817	0.850	0.865

SOURCE: Schlichting (36). Used with permission of the McGraw-Hill Companies.

Power law fit to velocity profile:

$$\frac{\overline{u}}{\overline{u}_{max}} = \left(1 - \frac{r}{r_o}\right)^m \qquad m = m(Re)$$

FIGURE 8.17   Exponent, n, for power-law velocity profiles.
(Adapted from Ref. 1.)

$$Re = \frac{\rho VD}{\mu}$$

FIGURE 8.18   Typical laminar flow and turbulent flow velocity profiles.

Viscous Distribution and Resistance – Rough Pipes

For laminar flow, effect of roughness is small; however, for turbulent flow the effect is large. Both laminar sublayer and overlap layer are affected.

Inner layer:

$$\bar{u} = \bar{u}\,(y, k, \rho, \tau_w)$$ not function of μ as was case for smooth pipe (or wall)

$$u^+ = u^+(y/k)$$

Outer layer: unaffected

Overlap layer:

$$u_R^+ = \frac{1}{\kappa}\ln\frac{y}{k} + \text{constant} \qquad\qquad \text{rough}$$

$$u_S^+ = \frac{1}{\kappa}\ln y^+ + B \qquad\qquad \text{smooth}$$

$$u_S^+ - u_R^+ = \underbrace{\frac{1}{\kappa}\ln k^+ + \text{constant}}_{\Delta B(k^+)} \qquad\qquad k^+ = \frac{ku^*}{\nu}$$

i.e., rough-wall velocity profile shifts downward by $\Delta B(k^+)$, which increases with k^+.

Three regions of flow depending on k^+

1. $k^+ < 5$ hydraulically smooth (no effect of roughness)
2. $5 < k^+ < 70$ transitional roughness (Re dependence)
3. $k^+ > 70$ fully rough (independent Re)

For 3, $\qquad \Delta B = \dfrac{1}{\kappa}\ln k^+ - 3.5 \qquad$ from data

$$u^+ = \frac{1}{\kappa}\ln\frac{y}{k} + 8.5 \neq f(Re)$$

$$\frac{V}{u^*} = 2.44\ln\frac{D}{k} + 3.2$$

$$\frac{1}{f^{1/2}} = -2\log\frac{k/D}{3.7}$$

fully rough flow

Composite Log-Law

$$u^+ = \overbrace{\frac{1}{\kappa}\ln y^+}^{\text{Smooth wall log law}} + \underbrace{B - \Delta B(k^+)}_{B^*}$$

$$B^* = 5 - \frac{1}{\kappa}\ln(1 + .3k^+) \qquad \text{from data}$$

$$\frac{1}{f^{1/2}} = -2\log\left[\frac{k/D}{3.7} + \frac{2.51}{Re\,f^{1/2}}\right] \qquad \text{Moody Diagram}$$

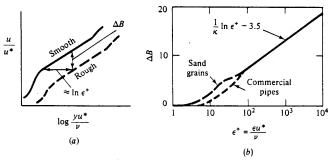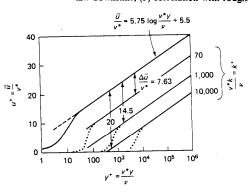$$= 1.14 - 2\log\left(\frac{k_s}{D} + \frac{9.35}{Re\,f^{1/2}}\right)$$

Fig. 6.12 Effect of wall roughness on turbulent pipe-flow velocity profiles: (a) logarithm-law downshift; (b) correlation with roughness
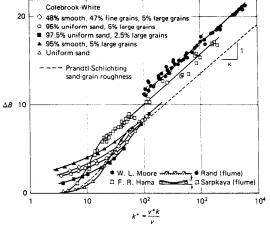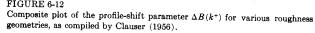

FIGURE 6-11
Experimental rough-pipe velocity profiles by Scholz (1955), showing the inward shift ΔB of the logarithmic overlap layer.

FIGURE 6-12
Composite plot of the profile-shift parameter $\Delta B(k^+)$ for various roughness geometries, as compiled by Clauser (1956).
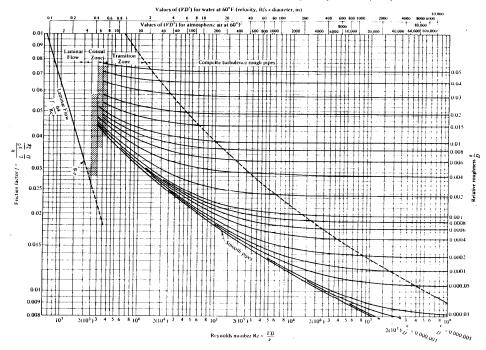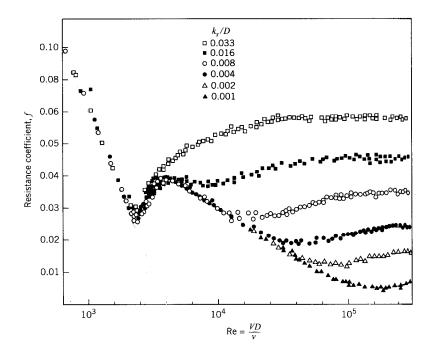

Fig. 6.13 The Moody chart for pipe friction with smooth and rough walls. (*From Ref. 8, by permission of the ASME.*)

FIGURE 10.7

Resistance coefficient
f *versus Re for sand-*
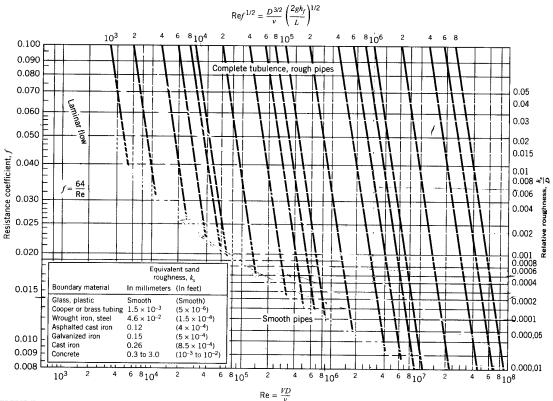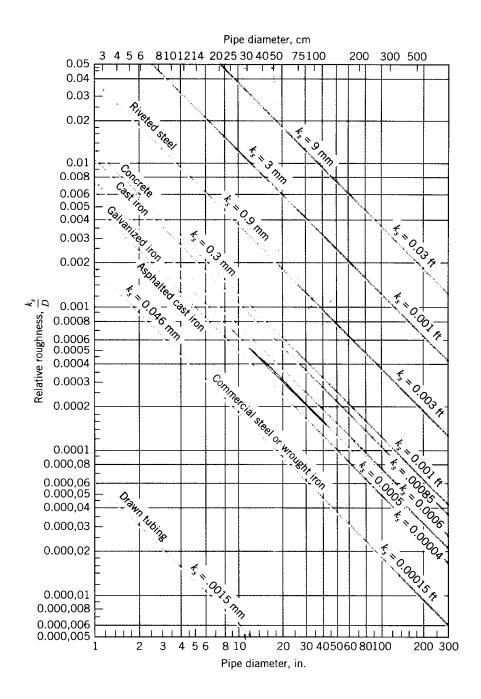*roughened pipe. [After*
Nikuradse (30)]

FIGURE 10.8

Resistance coefficient f
versus Re. Reprinted
with minor variations.
[After Moody (29).
Reprinted with
permission from the
A.S.M.E.]

FIGURE 10.9

Relative roughness for
various kinds of pipe.
[After Moody (29).
Reprinted with
permission from the
A.S.M.E.]

There are basically three types of problems involved with uniform flow in a single pipe:

1. Determine the head loss, given the kind and size of pipe along with the flow rate, $Q = A*V$
2. Determine the flow rate, given the head, kind, and size of pipe
3. Determine the pipe diameter, given the type of pipe, head, and flow rate

1. Determine the head loss

   The first problem of head loss is solved readily by obtaining f from the Moody diagram, using values of Re and k_s/D computed from the given data. The head loss h_f is then computed from the Darcy-Weisbach equation.

   $$f = f(Re_D, k_s/D)$$

   $$h_f = f \frac{L}{D} \frac{V^2}{2g} = \Delta h \qquad \Delta h = \left(\frac{p_1}{\gamma} + z_1\right) - \left(\frac{p_2}{\gamma} + z_2\right)$$

   $$= -\Delta\left(\frac{p}{\gamma} + z\right)$$

   $$Re_D = Re_D(V, D)$$

2. Determine the flow rate

   The second problem of flow rate is solved by trial, using a successive approximation procedure. This is because both Re and f(Re) depend on the unknown velocity, V. The solution is as follows:

1) solve for V using an assumed value for f and the Darcy-Weisbach equation

$$V = \left[\frac{2gh_f}{L/D}\right]^{1/2} \cdot f^{-1/2}$$

             known from   note sign

             given data

2) using V compute Re
3) obtain a new value for f = f(Re, k_s/D) and reapeat as above until convergence

Or can use $Re = f^{1/2} = \dfrac{D^{3/2}}{\nu}\left(\dfrac{2gh_f}{L}\right)^{1/2}$

scale on Moody Diagram

1) compute $Re f^{1/2}$ and k_s/D
2) read f
3) solve V from $h_f = f\dfrac{L}{D}\dfrac{V^2}{2g}$
4) Q = VA

3. Determine the size of the pipe

The third problem of pipe size is solved by trial, using a successive approximation procedure. This is because h_f, f, and Q all depend on the unknown diameter D. The solution procedure is as follows:

1) solve for D using an assumed value for f and the Darcy-Weisbach equation along with the definition of Q

$$D = \left[\frac{8LQ^2}{\pi^2 g h_f} \right]^{1/5} \cdot f^{1/5}$$

$\underbrace{\phantom{\frac{8LQ^2}{\pi^2 g h_f}}}$

known from given data

2) using D compute Re and k_s/D

3) obtain a new value of $f = f(Re, k_s/D)$ and reapeat as above until convergence

Flows at Pipe Inlets and Losses From Fittings

For real pipe systems in addition to friction head loss these are additional so called minor losses due to

1. entrance and exit effects
2. expansions and contractions
3. bends, elbows, tees, and other fittings
4. valves (open or partially closed)

can be large effect

For such complex geometries we must rely on experimental data to obtain a loss coefficient

$$K = \frac{h_m}{\dfrac{V^2}{2g}}$$ ← head loss due to minor losses

In general,

$$K = K(\text{geometry, Re, } \varepsilon/D)$$
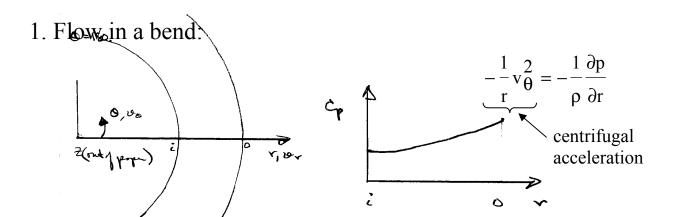
dependence usually
not known

Loss coefficient data is supplied by manufacturers and also listed in handbooks. The data are for turbulent flow conditions but seldom given in terms of Re.

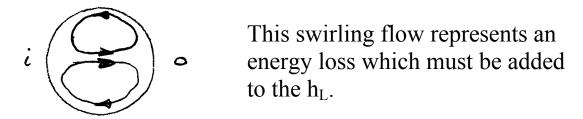Modified Energy Equation to Include Minor Losses (where $V = \overline{V}$):

$$\frac{p_1}{\gamma} + z_1 + \frac{1}{2g}\alpha_1 V_1^2 + h_p = \frac{p_2}{\gamma} + z_2 + \frac{1}{2g}\alpha_2 V_2^2 + h_t + h_f + \sum h_m$$
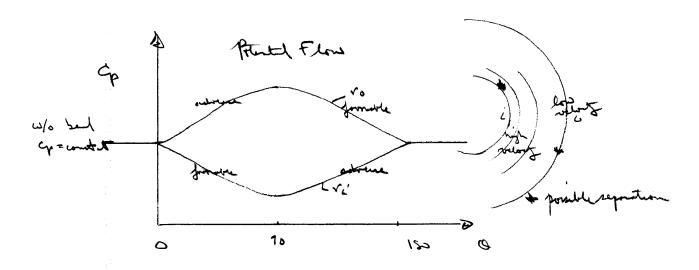
$$h_m = K\frac{V^2}{2g}$$

Note: Σh_m does not include pipe friction and e.g. in elbows and tees, this must be added to h_f.

1. Flow in a bend:

$$-\frac{1}{r}v_\theta^2 = -\frac{1}{\rho}\frac{\partial p}{\partial r}$$
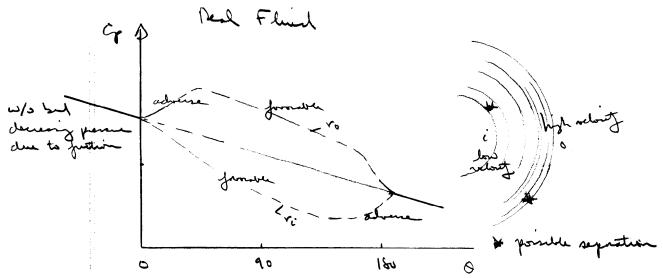
centrifugal acceleration

i.e. $\dfrac{\partial p}{\partial r} > 0$ which is an adverse pressure gradient in r
direction. The slower moving fluid near wall responds first
and a swirling flow pattern results.

This swirling flow represents an
energy loss which must be added
to the h_L.

Also, flow separation can result due to adverse longitudinal
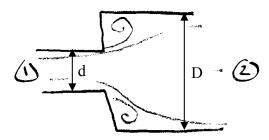pressure gradients which will result in additional losses.

This shows potential flow is not a good approximate in
internal flows (except possibly near entrance)

2. Valves: enormous losses

3. Entrances: depends on rounding of entrance

4. Exit (to a large reservoir): K = 1
   i.e., all velocity head is lost

5. Contractions and Expansions
   sudden or gradual

   theory for expansion:

$$h_L = \frac{(V_1 - V_2)^2}{2g}$$

from continuity, momentum, and energy

(assuming $p = p_1$ in separation pockets)

$$\Rightarrow \quad K_{SE} = \left(1 - \frac{d^2}{D^2}\right)^2 = \frac{h_m}{V_1^2 \Big/ 2g}$$

no theory for contraction:

$$K_{SC} = .42\left(1 - \frac{d^2}{D^2}\right)$$

vena contracta

from experiment

If the contraction or expansion is gradual the losses are quite different. A gradual expansion is called a diffuser. Diffusers are designed with the intent of raising the static pressure.

$$C_p = \frac{p_2 - p_1}{\frac{1}{2}\rho V_1^2}$$

$$C_{p_{ideal}} = 1 - \left(\frac{A_1}{A_2}\right)^2 \qquad \text{Bernoulli and continuity equation}$$

$$K = \frac{h_m}{V^2 \Big/ 2g} = C_{p_{ideal}} - C_p \quad \text{Energy equation}$$

Actually very complex flow and

$$C_p = C_p \text{ (geometry, } \underbrace{\text{inlet flow conditions)}}$$

i.e., fully developed (long pipe) reduces C_p
thin boundary layer (short pipe) high C_p
(more uniform inlet profile)

FIGURE 10.10

*Flow characteristics at a
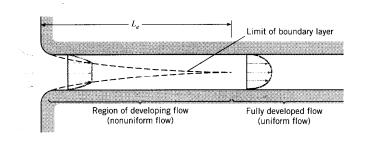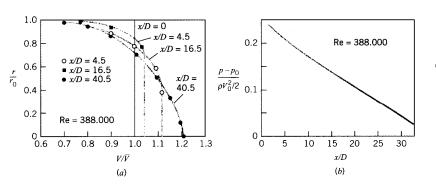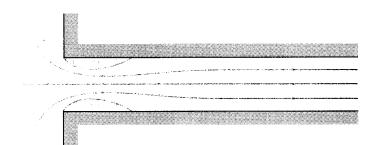pipe inlet (not to scale).*

L_e

Limit of boundary layer

Region of developing flow   Fully developed flow
(nonuniform flow)   (uniform flow)

FIGURE 10.11

*Distribution of velocity
and pressure in the inlet
region of a pipe [Barbin
and Jones (3)].*
(a) Velocity distribution.
(b) Pressure distribution.

$x/D = 0$
$x/D = 4.5$
$x/D = 16.5$

o $x/D = 4.5$
■ $x/D = 16.5$
● $x/D = 40.5$

$x/D = 40.5$

Re = 388.000

$\frac{r}{r_0}$

$V/\bar{V}$

(a)

$\frac{p - p_0}{\rho V_0^2/2}$

Re = 388.000

x/D

(b)

Turbulent
flow

FIGURE 10.12

*Flow at a sharp-edged
inlet.*

K = .5

FIGURE 10.13

Flow pattern in an elbow.

Separation zone

See textbook Table 8.2 for a table of the loss coefficients for pipe components

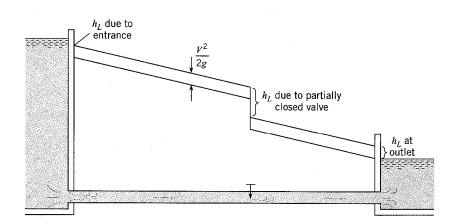TABLE 10.2   LOSS COEFFICIENTS FOR VARIOUS TRANSITIONS AND FITTINGS

Description	Sketch	Additional Data		K	Source
Pipe entrance $h_L = K_e V^2/2g$		r/d 0.0 0.1 >0.2		K_e 0.50 0.12 0.03	(2)*
Contraction $h_L = K_C V_2^2/2g$		D_2/D_1 0.0 0.20 0.40 0.60 0.80 0.90	K_C $\theta = 60°$ 0.08 0.08 0.07 0.06 0.06 0.06	K_C $\theta = 180°$ 0.50 0.49 0.42 0.27 0.20 0.10	(2)
Expansion $h_L = K_E V_1^2/2g$		D_1/D_2 0.0 0.20 0.40 0.60 0.80	K_E $\theta = 20°$ 0.30 0.25 0.15 0.10	K_E $\theta = 180°$ 1.00 0.87 0.70 0.41 0.15	(2)
90° miter bend	Vanes	Without vanes	$K_b = 1.1$		(37)
		With vanes	$K_b = 0.2$		(37)
90° smooth bend		r/d 1 2 4 6 8 10	$K_b = 0.35$ 0.19 0.16 0.21 0.28 0.32		(5) and (19)
Threaded pipe fittings	Globe valve—wide open Angle valve—wide open Gate valve—wide open Gate valve—half open Return bend Tee straight-through flow side-outlet flow 90° elbow 45° elbow	$K_v = 10.0$ $K_v = 5.0$ $K_v = 0.2$ $K_v = 5.6$ $K_b = 2.2$ $K_t = 0.4$ $K_t = 1.8$ $K_b = 0.9$ $K_b = 0.4$			(37)

*Reprinted by permission of the American Society of Heating, Refrigerating and Air Conditionii
Engineers, Atlanta, Georgia, from the 1981 ASHRAE Handbook-Fundamentals.

FIGURE 10.14

EGL and HGL at a sharp-edged pipe entrance.

Steeper gradient in the EGL due to turbulence produced at the entrance

$\dfrac{V^2}{2g}$

EGL

Drop in the HGL due to high velocity in flow just downstream of entrance

HGL

IGURE 10.15

ead losses in a pipe.

h_L due to entrance

$\dfrac{V^2}{2g}$

h_L due to partially closed valve

h_L at outlet